

Physics of Semiconductors (6)

Shingo Katsumoto
Institute for Solid State Physics, University of Tokyo

August 15, 2013

7.2.3 k·p perturbation

k·p perturbation is an adequate method to obtain highly accurate band structures around band edges. Though in empirical pseudo potential method we can reproduce band structure from very few parameters with comparatively simple calculation, in k·p perturbation we need to increase the number of bands included in the calculation, which increases the dimension of matrices and large scale calculation is required.

The basics of k·p perturbation is eq.(1.4) in the first hour of this lecture. Substituting Bloch function $e^{i\mathbf{k}\mathbf{r}}u_{n\mathbf{k}}(\mathbf{r})$ into the original Schrödinger equation, we obtain the equation for the lattice periodic part $u_{n\mathbf{k}}(\mathbf{r})$. In three dimensional space (1.4) can be written as

$$\left[-\frac{\hbar^2 \nabla^2}{2m_0} + V(\mathbf{r}) + \frac{\hbar^2 \mathbf{k}^2}{2m_0} - i \frac{\hbar^2}{m_0} \mathbf{k} \cdot \nabla \right] u_{n\mathbf{k}}(\mathbf{r}) = E_{n\mathbf{k}} u_{n\mathbf{k}}(\mathbf{r}). \quad (6.1)$$

Here the Bloch wavenumber \mathbf{k} is a parameter (c-number) and not an operator.

Now we redefine the unperturbed Hamiltonian \mathcal{H}_0 and \mathbf{k} -dependent eigen energy as

$$\mathcal{H}_0 \equiv -\frac{\hbar^2 \nabla^2}{2m_0} + V(\mathbf{r}), \quad E'_n(\mathbf{k}) = E_{n\mathbf{k}} - \frac{\hbar^2 \mathbf{k}^2}{2m_0}.$$

Then the perturbation term can be written as

$$\mathcal{H}'(\mathbf{k}) = -i \frac{\hbar^2}{m_0} \mathbf{k} \cdot \nabla = \frac{\hbar}{m_0} \mathbf{k} \cdot \hat{\mathbf{p}}, \quad (6.2)$$

from which we can easily guess the source of the naming “k·p”.

(6.2) is zero for $\mathbf{k} = 0$. Hence we set the unperturbed state as $\mathbf{k} = 0$. Assume that we obtain the exact eigenstates $\{u_{j0}(\mathbf{r})\}$ for $\mathbf{k} = 0$, then they form a complete set and an eigenstate for finite \mathbf{k} can be expanded as

$$u_{n\mathbf{k}}(\mathbf{r}) = \sum_{j=0}^{\infty} c_{nj}(\mathbf{k}) u_{j0}(\mathbf{r}).$$

These $c_{nj}(\mathbf{k})$ can be obtained from the perturbation of $\mathcal{H}'(\mathbf{k})$. This is the concept of k·p perturbation.

In the above $\mathbf{k} = 0$ is taken to the unperturbed point assuming some avoided level crossing due to the high symmetry. Such avoided level crossing results in $\partial E / \partial k = 0$ and the approximation is practically good around the point because $\mathcal{H}'(\mathbf{k})$ is small around it. Similar may occur in other points with high symmetry and k·p expansions around such points are also available. Also as we have seen so far, physical properties of semiconductors are determined with band structures around such symmetric points. We cannot perform, of course, the infinite summation hence cut the summation around the band n which is under consideration. The accuracy of the k·p perturbation usually determined by the number of bands taken into account.

(a) the case of non-degenerate $u_{i0}(\mathbf{r})$

$$u_{i\mathbf{k}}(\mathbf{r}) = u_{i0}(\mathbf{r}) + \sum_{j \neq i} \frac{\langle j | \mathcal{H}' | i \rangle}{E_i - E_j} u_{j0}(\mathbf{r}), \quad E_i(\mathbf{k}) = E_i(0) + \langle i | \mathcal{H}' | i \rangle + \sum_{j \neq i} \frac{|\langle i | \mathcal{H}' | j \rangle|^2}{E_i - E_j} \quad (6.3)$$

are obtained as the first order perturbation. Here we have used abbreviation $|i\rangle$ for $|u_{i0}(\mathbf{r})\rangle$. From $\langle i|j\rangle = \delta_{ij}$ and $\langle i|\nabla|i\rangle = 0$,

$$E_i(\mathbf{k}) = E_i(0) + \frac{\hbar^2 \mathbf{k}^2}{2m_0} - \frac{\hbar^4}{m_0^2} \sum_{j \neq i} \frac{\langle i|\mathbf{k} \cdot \nabla|j\rangle \langle j|\mathbf{k} \cdot \nabla|i\rangle}{E_i - E_j}. \quad (6.4)$$

(b) the case $u_{i0}(\mathbf{r})$ has degeneracy

When $u_{00}(\mathbf{r})$ has n -fold degeneracy, we take an orthogonal basis $\{u_{00}^j(\mathbf{r})\}$ ($j = 1, \dots, n$) and write the functions in short form as $|0j\rangle$. Perturbed wavefunction is approximated with the linear combination $|u_{0\mathbf{k}}^i\rangle = \sum_{j=1}^n A_{ij}(\mathbf{k})|0j\rangle$. Substituting this into (6.1) gives $[\mathcal{H}_0 + \mathcal{H}' - E_0(\mathbf{k})]u_{0\mathbf{k}} = 0$. With taking inner product with $|0i\rangle$, equation

$$\sum_{j=1}^n A_{ij}(\mathbf{k}) [\langle 0i|\mathcal{H}_0|0j\rangle + \langle 0i|\mathcal{H}'_0|0j\rangle - \langle 0i|E_0(\mathbf{k})|0j\rangle] \\ = \sum_{j=1}^n A_{ij}(\mathbf{k}) [\langle 0i|\mathcal{H}'|0j\rangle + (E_0 - E_0(\mathbf{k}))\delta_{ij}] = 0 \quad (6.5)$$

is obtained. The secular equation for this simultaneous equation to have non-trivial solution is

$$|\langle 0i|\mathcal{H}'|0j\rangle + (E_0 - E_0(\mathbf{k}))\delta_{ij}| = 0, \quad (6.6)$$

which gives the dispersion relation $E_0(\mathbf{k})$. From the solution $A_{ij}(\mathbf{k})$, we obtain approximate set of eigenfunctions corresponding to \mathbf{k} .

7.2.4 Spin-orbit interaction

For rigorous derivation of **spin-orbit interaction** we should go back to Dirac equation, for which we do not have enough time unfortunately. Here without any derivation, we adopt the Hamiltonian for spin-orbit interaction as

$$\mathcal{H}_{\text{so}} = -\frac{\hbar}{4m_0^2 c^2} \boldsymbol{\sigma} \cdot \mathbf{p} \times (\nabla V). \quad (6.7)$$

And just discuss the effect on the band structure. $\boldsymbol{\sigma} = (\sigma_x, \sigma_y, \sigma_z)$ is a vector which has Pauli matrices:

$$\sigma_x = \begin{pmatrix} 0 & 1 \\ 1 & 0 \end{pmatrix}, \quad \sigma_y = \begin{pmatrix} 0 & -i \\ i & 0 \end{pmatrix}, \quad \sigma_z = \begin{pmatrix} 1 & 0 \\ 0 & -1 \end{pmatrix}, \quad (6.8)$$

as its elements. (6.7) is added to (6.1) and with (1.5), we obtain

$$\left[\frac{p^2}{2m_0} + V + \frac{\hbar^2 k^2}{2m_0} + \frac{\hbar}{m_0} \mathbf{k} \cdot \boldsymbol{\pi} + \frac{\hbar}{4m_0^2 c^2} \mathbf{p} \cdot \boldsymbol{\sigma} \times \nabla V \right] |n\mathbf{k}\rangle = E_n(\mathbf{k})|n\mathbf{k}\rangle, \\ \boldsymbol{\pi} \equiv \mathbf{p} + \frac{\hbar}{4m_0 c^2} \boldsymbol{\sigma} \times \nabla V. \quad (6.9)$$

We expand the solution, again with the basis of the band bottom $|\nu 0\rangle$. This time we need to take care of spin freedom and write $|\nu, \sigma\rangle \equiv |\nu 0\rangle \otimes |\sigma\rangle$, and expand as $|n\mathbf{k}\rangle = \sum_{\nu', \sigma'} c_{n\nu'\sigma'} |\nu', \sigma'\rangle$. With taking inner product with $\langle \nu, \sigma|$, we obtain the eigen equation as

$$\sum_{\nu', \sigma'} \left\{ \left[E_{\nu'}(0) + \frac{\hbar^2 k^2}{2m} \right] \delta_{\nu\nu'} \delta_{\sigma\sigma'} + \frac{\hbar}{m} \mathbf{k} \cdot \mathbf{P}_{\sigma\sigma'}^{\nu\nu'} + \Delta_{\sigma\sigma'}^{\nu\nu'} \right\} c_{n\nu'\sigma'} = E_n(\mathbf{k}) c_{n\nu\sigma}. \quad (6.10)$$

where

$$\mathbf{P}_{\sigma\sigma'}^{\nu\nu'} \equiv \langle \nu\sigma|\boldsymbol{\pi}|\nu'\sigma'\rangle, \quad \Delta_{\sigma\sigma'}^{\nu\nu'} \equiv \frac{\hbar^2}{4m^2 c^2} \langle \nu\sigma|[\mathbf{p} \cdot \boldsymbol{\sigma} \times (\nabla V)]|\nu'\sigma'\rangle. \quad (6.11)$$

The dispersion relation again is obtained with solving the eigen value problem. In this stage, it is often a good approximation to drop the spin-orbit part. In such cases it can be written as $\boldsymbol{\pi} = \mathbf{p}$, $\mathbf{P}_{\sigma\sigma'}^{\nu\nu'} = \delta_{\sigma\sigma'} \mathbf{P}_{\nu\nu'}$.

7.2.5 Wavefunctions at Γ -point in fcc semiconductors

In empirical $k \cdot p$ method, without detailed knowledge of wavefunctions, the parameters required for the band calculation are extracted theoretically and the values are obtained from experiments. Many of such parameters are zero around highly symmetrical points making the calculation easier. Hence the knowledges of spatial symmetries in crystal and in atomic orbitals are important. Though the theory of space group gives systematic discussion to this problem, again due to the time limitation, we restrict ourselves to the discussion around Γ -point in fcc semiconductors.

Bravais lattice is fcc for group IV semiconductors with diamond structure and group III-V semiconductors with zinc blende structure. Here we name them ‘‘DZB’’ semiconductors. As is guessed from the structure in Fig.5.10(b), in chemical bond theory the crystal formation can be understood along covalent bonding between neighboring sp^3 hybrid orbitals. In the group III-V semiconductors, for each atom to form sp^3 hybrid, it needs to be ionized. Hence the crystals are also formed with the ionic bonding. The most effective atomic orbitals on the band structures in these semiconductors are s and p . In DZB structure, there are two atoms per a single lattice point in the simplest fcc structure (Fig.5.10). In Fig.5.9, substituting $2 \times 4 = 8$ into Z , we see that the energy gap opens around the degeneracy points in the distance around $\sqrt{3}$ from Γ point.

We consider a function $|S\rangle$, which has the lattice translational symmetry though also has the same angular symmetry as s orbital in the vicinities of nuclei. For that, we first take a linear combination of atomic orbitals (LCAO) of s orbital $|s\rangle$

$$|u_s\rangle = \sum_{i,\beta} a_{i\beta} |s_{i\beta}\rangle,$$

where i is the index of unit cells, β is the relative index of atoms in a unit cell (as is in the pseudo potential calculation). Though the above function satisfies the crystal translational symmetry, it is not a solution for the Schrödinger equation with lattice potential. Hence we assume that we can modify the form of $|s\rangle$ to make the linear combined function a solution for the Schrödinger equation with keeping the rotational symmetry in $|s\rangle$ characteristic to the s -orbital. We write thus obtained LCAO wavefunction as $|S\rangle$, which must satisfy

$$\mathcal{H}_0|S\rangle = \left[-\frac{\hbar^2 \nabla^2}{2m_0} + V(\mathbf{r}) \right] |S\rangle = E_c|S\rangle. \quad (6.12)$$

In the same way we define $|X\rangle$, $|Y\rangle$, $|Z\rangle$, which have angular symmetries of p_x , p_y , p_z respectively around nuclei, translational symmetry at the same time.

At Γ -point, the bottom of conduction band is mostly made from s orbitals while the top p orbitals. Hence, though the approximation is rough, we assume the above defined functions satisfy the unperturbed ($\mathbf{k} = 0$) equation

$$\mathcal{H}_0|\zeta\rangle = \left[-\frac{\hbar^2 \nabla^2}{2m_0} + V(\mathbf{r}) \right] |\zeta\rangle = E_b|\zeta\rangle, \quad (6.13)$$

where $\zeta \in \{S, X, Y, Z\}$, E_b is E_c for $\zeta = S$ and E_v for others. It may be a problem whether such functions as $|S\rangle$, $|X\rangle$, \dots actually exist. The space group theory says we can adopt lattice periodic functions with the same angular symmetries as s or p_α orbitals around the point at which parabola with bottoms at $(\pm 1, \pm 1, \pm 1)$ degenerate in the empty lattice approximation.¹

For the convenience to take into account the spin-orbit interaction, we transform basis from $|X\rangle$, $|Y\rangle$, $|Z\rangle$ to

$$|+\rangle \equiv (|X\rangle + i|Y\rangle)/\sqrt{2}, \quad |0\rangle \equiv |Z\rangle, \quad |-\rangle \equiv (|X\rangle - i|Y\rangle)/\sqrt{2},$$

which correspond to eigen functions of angular momentum $|p_{+1}\rangle$, $|p_0\rangle$, $|p_{-1}\rangle$ respectively. With the direct product of these four basis functions for the orbital part and two for the spin part (\uparrow, \downarrow), eight basis functions in total, roughest $k \cdot p$ perturbation calculation, in which the orbital degeneracy and the spin-orbit interaction are taken into account can be performed.

¹e.g. see Inui, Tanabe, Onodera, ‘‘Applied group theory’’ (Shokabo, 1976) Chapter 11 (in Japanese).

The perturbation Hamiltonian to $|n\mathbf{k}\rangle$ is taken as

$$\mathcal{H}' + \mathcal{H}_{\text{SO}} = -i\frac{\hbar^2}{m_0}\mathbf{k} \cdot \nabla - \frac{\hbar}{4m_0^2c^2}\boldsymbol{\sigma} \cdot (\mathbf{p} \times \nabla V), \quad (6.14)$$

in which we have dropped higher order terms from (6.9) and put $\boldsymbol{\pi} = \mathbf{p}$. The matrix elements between $|S\rangle$, $|X\rangle, \dots$ are

$$P \equiv \frac{\hbar}{m_0}\langle S|p_x|X\rangle = \frac{\hbar}{m_0}\langle S|p_y|Y\rangle = \frac{\hbar}{m_0}\langle S|p_z|Z\rangle, \quad (6.15)$$

$$\Delta \equiv -\frac{3i\hbar}{4m_0^2c^2}\langle X|[\nabla V \times \mathbf{p}]_y|Z\rangle = (\text{cyclic replacement of } xyz) \quad (6.16)$$

and their conjugate elements. Others are zero due to the symmetries around nuclei.

Hence non-zero matrix elements of \mathcal{H}' are

$$\langle S\alpha|\mathcal{H}'|0\alpha'\rangle = Pk_z\delta_{\alpha\alpha'}, \quad \langle S\alpha|\mathcal{H}'|\pm\alpha'\rangle = \frac{\mp P}{\sqrt{2}}(k_x \pm ik_y)\delta_{\alpha\alpha'}, \quad (6.17)$$

and their conjugate elements $\mathcal{H}'_{ji} = (\mathcal{H}'_{ij})^*$, where α, α' are spin coordinates. As for \mathcal{H}_{SO} ,

$$\begin{aligned} \langle \pm\uparrow|\mathcal{H}_{\text{SO}}|\pm\uparrow\rangle &= -\langle \pm\downarrow|\mathcal{H}_{\text{SO}}|\pm\downarrow\rangle = \pm\Delta/3, \\ \langle \pm\alpha|\mathcal{H}_{\text{SO}}|0\alpha'\rangle &= (1 - \delta_{\alpha\alpha'})\sqrt{2}\Delta/3, \end{aligned} \quad (6.18)$$

and others are zero. From (6.13), unperturbed Hamiltonian \mathcal{H}_0 has

$$\langle S\alpha|\mathcal{H}_0|S\alpha'\rangle = \delta_{\alpha\alpha'}E_c, \quad \langle \{+, 0, -\}\alpha|\mathcal{H}_0|\{+, 0, -\}\alpha'\rangle = \delta_{\alpha\alpha'}E_v. \quad (6.19)$$

From the above we obtain the secular equation and thus the energy eigen values $E_n(\mathbf{k})$. \mathcal{H}' is an 8×8 matrix in the present basis though if we fix the wavenumber vector to z direction, i.e., $\mathbf{k} = (0, 0, k)$, it becomes

$$\begin{bmatrix} H_d & 0 \\ 0 & H_d \end{bmatrix},$$

thus is broken down to 4×4 matrices and

$$H_d = \begin{bmatrix} E_c & 0 & kP & 0 \\ 0 & E_v - \Delta/3 & \sqrt{2}\Delta/3 & 0 \\ kP^* & \sqrt{2}\Delta/3 & E_v & 0 \\ 0 & 0 & 0 & E_v + \Delta/3 \end{bmatrix}. \quad (6.20)$$

From this the secular equation to obtain the eigenvalue λ is obtained as

$$\begin{aligned} \lambda &= E_v + \frac{\Delta}{3}, \\ (\lambda - E_c) \left(\lambda - E_v + \frac{2\Delta}{3} \right) \left(\lambda - E_v - \frac{\Delta}{3} \right) - |P|^2k^2 \left(\lambda - E_v + \frac{\Delta}{3} \right) &= 0. \end{aligned}$$

In the second equation we approximate that the term of $|P|^2k^2$ is small then obtain the energies for the conduction band $E_c(\mathbf{k})$, and the valence band $E_{vj}(\mathbf{k})$ as

$$E_c(\mathbf{k}) = E_c + \frac{\hbar^2k^2}{2m} + \frac{|P|^2k^2}{3} \left[\frac{2}{E_g} + \frac{1}{E_g + \Delta} \right], \quad (6.21)$$

$$E_{v1}(\mathbf{k}) = E_v + \frac{\Delta}{3} + \frac{\hbar^2k^2}{2m_0}, \quad (6.22)$$

$$E_{v2}(\mathbf{k}) = E_v + \frac{\Delta}{3} + \frac{\hbar^2k^2}{2m_0} - \frac{2|P|^2k^2}{3E_g}, \quad (6.23)$$

$$E_{v3}(\mathbf{k}) = E_v - \frac{2\Delta}{3} + \frac{\hbar^2k^2}{2m_0} - \frac{|P|^2k^2}{3(E_g + \Delta)}. \quad (6.24)$$

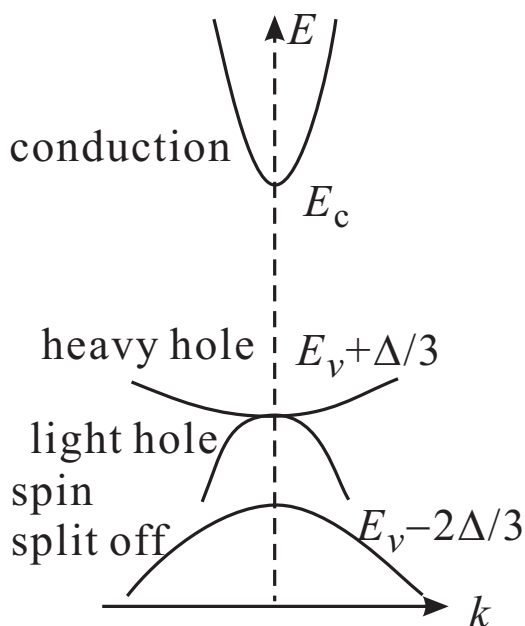


Figure 6.1: Band structure for diamond and zinc blende semiconductors calculated from the lowest order k-p perturbation with adopting only S and P orbitals. Spin-orbit splitting exists though the heavy hole mass is the same as that of the vacuum electron, that is, the hole mass is negative in this calculation.

The band structure around $k = 0$ thus far obtained is displayed in Fig.6.1. Small mass of the conduction band, two different masses at the top of the valence band, and lowered energy of spin split-off band due to the spin-orbit coupling in the valence band, which properties are well known from optical measurements, cyclotron measurements, etc, are reproduced qualitatively though in particular, the heavier valence band mass is that of the vacuum electron, that is, the hole effective mass is predicted to be negative apparently different from the real band structure. This is, of course, due to the coarse approximation, which is to the first order perturbation based on the degenerate four bands. The accuracy is enhanced by enhancing the order of perturbation to second, and by taking the surrounding bands into account. At present front of calculation, due to algorithm developments, and enhancement in computational performance have made it possible to perform calculations including over 20 bands and results with high accuracy which can be even used at comparatively high k [1].

Another way to utilize the result of k-p “empirically” is, as is in the pseudo potential method, to represent the results of second order k-p perturbation with a small number of parameters (*e.g.* Luttinger parameters) and to determine them fitting to the experiments. In the case of valence band in diamond and zinc blende semiconductors, the energies can be expressed as

$$E_v(\mathbf{k}) = E_v + \frac{\Delta}{3} + Ak^2 \pm \sqrt{B^2k^4 + C^2(k_x^2k_y^2 + k_y^2k_z^2 + k_z^2 + k_x^2)}, \quad (6.25)$$

$$E_{vsp}(\mathbf{k}) = E_v - \frac{2\Delta}{3} + Ak^2, \quad (6.26)$$

and A, B, C are obtained from, *e.g.* cyclotron resonance.

8 Electronic states in organic semiconductors

Knowledges on general properties of inorganic semiconductors were rapidly established from around 1950s due to the development in synthesis and theories and have been expanded so far. Despite developments of many new concepts and novel experimental methods, what had been once established have not received fatal corrections. On the other hand in the case of organic semiconductors, it is very difficult to make definitive statements on many important physical properties. Because the qualities of materials in the initial stage for the usage of organics as semiconductors were so low, many oversimplification has been made to explain many mysterious results. Some successes had been attained though many of them were rewritten or discarded when there were significant improvement in the quality of materials. And the qualities or the methods for the synthesis are still not satisfactory, in other words, there is still a big room for the improvement.

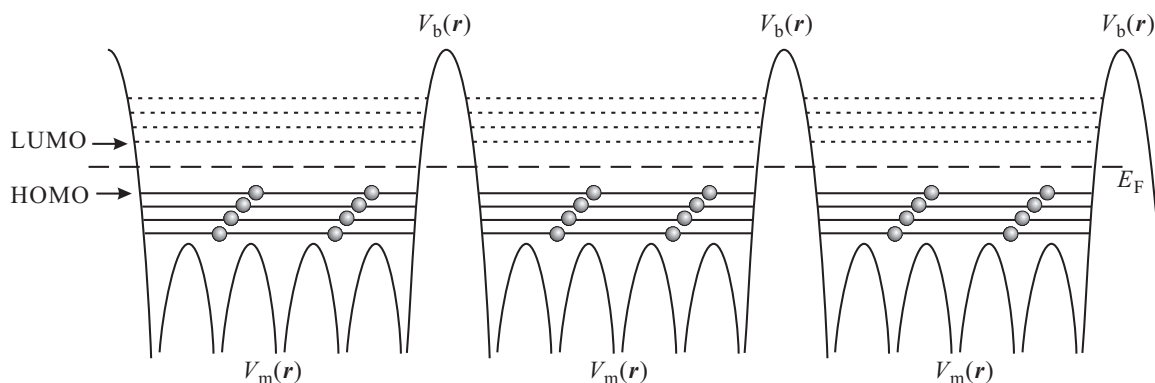


Figure 6.2: Schematic view of electronic states in bulk organic semiconductors

For example, many textbooks on organic semiconductors say “it is impossible, generally, to control p-type or n-type in organic semiconductors with chemical doping”[2] though very recently, it has been found that with a simple method called “co-evaporation”, n- and p-types can be freely controlled. Or it has also been said that ionization energies can be accurately measured with photoelectron emission spectroscopy but it is very difficult to determine the spatial modulation of electronic bands. (Even the former statement had not been common sense until the photoelectron emission spectroscopy had become so common method.) However in these one, two years, it has become possible to measure the spatial modulation of band edges with so called Kelvin probe method, which is an application of the STM technique.

Hence, here we have a coarse look at “present” concepts on the electronic states in organic semiconductors.

8.1 Organic semiconductor materials

Many of the organic semiconductors are ensembles of molecules loosely coupled with van der Waals force, which are so called molecular crystals. Inside the molecules, the atoms are tightly bound with covalent bonding and electrovalent bonding. When the size of molecules is huge as polymers, the potentials inside the molecules can be treated as spatially periodic ones, and thus the energy band theory for periodic crystal lattices is applicable. In the case of middle size molecules, **molecular orbitals** can be defined inside the molecules and the intra-molecule transfer of electrons occurs through the molecular orbitals.

The molecules are of the same species inside the materials, so are the molecular orbitals. Due to the finite size of molecules, the energy spectra are discrete. At absolute zero, the orbital levels below the Fermi level, E_F of each molecule, are occupied with electrons and those above E_F are empty. The molecular orbital that has the highest energy among the occupied levels, is called **HOMO** in the abbreviation of highest occupied molecular orbital, and the one that has the lowest among the empty levels, is called **LUMO** in the abbreviation of lowest unoccupied molecular orbital².

On the other hand, the couplings between the molecules are weak and the periodicities are often greatly disordered though some of the materials still have good spatial periodicity. In the materials with spatial periodicity, HOMO and LUMO form energy band though the widths are so narrow due to the small hopping integral (1.14). Summing up the above, the diagrams like displayed in Fig.6.2 are often adopted for the representation of electronic states in organic semiconductors.

8.2 Electronic transport in organic semiconductors

From Fig.6.2, we can deduce that the organic semiconductors, as are in non-organic ones, are generally insulating. Furthermore, we suspect that even we have some extra electrons in LUMO with *e.g.* chemical doping, the electric conduction would be dominated by **hopping conduction**, in which the electrons go over the potentials between the molecules $V_b(r)$ with thermal activation, in other words, we cannot expect metallic transport.

²These terms were introduced by Ken-ichi Fukui[3]

However, in actual cases, in some organic materials, the electric conductivities go up with orders of magnitude with doping. A well known example is, polyacetylene, the main finding of Hideki Shirakawa to which the Nobel prize of chemistry was given. In this case, a polyacetylene is made of polymers and one-dimensional bands are formed inside the molecules and a kind of “impurity bands” should be formed even inside the molecules because they contact each other with very long distances though the couplings themselves are weak. These properties result in such metallic conduction. The academic interests in polyacetylene lie mainly in one dimensional conduction through the polymers as are in the cases of TTF-TCNQ or (TMTSF)₂PF₆, which shows superconductivity,³ such as the transport of topological solitons[5]. These materials show many interesting phenomena concerning with so called strongly correlated physics, such as charge density waves (CDWs) or orbital ordering.

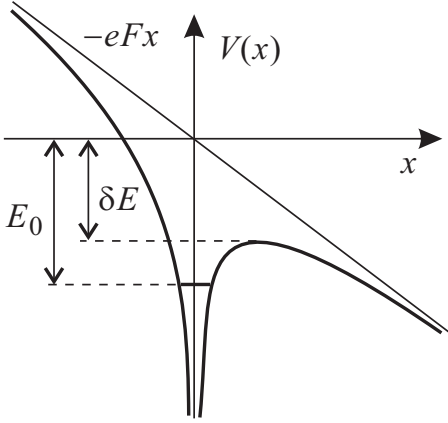


Figure 6.3: Illustration of an energy diagram, in which an external electric field is applied to a trap potential of electrons. The effective activation energy is lowered by the field.

When the thermally activated mobility at zero electric field is given as $\mu(0) = \mu_0 \exp(-E_0/k_B T)$, it changes with electric field F due to the shift of the activation energy to $E_0 - \delta E$ as

$$\mu(F) = \mu_0 \exp\left[-\frac{E_0 - \delta E}{k_B T}\right] = \mu(0) \exp\left[\frac{\delta E}{k_B T}\right] \equiv \mu(0) \exp(\beta(T) F^{1/2}), \quad (6.29)$$

where $\beta(T)$ is called Poole-Frenkel coefficient written as

$$\beta(T) = (e^3/\pi\epsilon\epsilon_0)^{1/2}/k_B T. \quad (6.30)$$

Equation (6.29) well explains some experimental results. This model is, however, based on the hypothesis that the trap potentials distribute with complete randomness, *i.e.* the coherence is completely lost. The mobilities in organic semiconductors have risen by 5 orders of magnitude though the rate has a bit fallen in these 8 years. And in near future we may be released from the Poole-Frenkel model or the polarons in the bulk transport.

Besides such metallic examples, as we first expected in many organic semiconductors, the weak couplings between the molecules determine the transport characteristics. We thus need to treat electric transport of such “half-localized” electrons. A simplest traditional model for such conduction in insulators under finite electric field is Poole-Frenkel model, which is illustrated in Fig.6.3. When a carrier is trapped in a potential with the activation energy E_0 , the applied field F lowers the energy by δE for the direction along the field.

In Fig.6.3 we assume a Coulomb type trapping potential,

$$V(r) = -\frac{e^2}{4\pi\epsilon\epsilon_0 r} - eFx. \quad (6.27)$$

E_0 can be estimated as the Rydberg constant with dielectric constant ϵ and δE is obtained from the condition of inflection point as

$$\delta E = \sqrt{\frac{e^3 F}{\pi\epsilon\epsilon_0}}. \quad (6.28)$$

³See *e.g.* [4], to know the molecular structure of these organic materials.

Ch. 3 Semiconductor electronic devices

In this chapter we begin the discussion on physical phenomena in spatially non-uniform structures of semiconductors and see how they are applied to the devices for electronic circuits or light emission/detection. And also see how they can be used for quantum structures.

1 PN junctions

1.1 Equilibrium condition

Connected structure of p-type and n-type semiconductors is a pn junction. Here we only consider homo-junctions, in which the same species semiconductor is used for p and n layers. As we saw in Appendix 1, an n-type layer has many electrons, while a p-type has many holes, there should be some driving forces in entropy part of the free energy that the diffusion of electrons from n to p, the inverse for holes. In equilibrium, the diffusion should be balanced with the force from the electric field driven by the electric polarization at the interface caused by the diffusions. In other words, the free energy which is the sum of the internal energy U and the negative product of the temperature T and the entropy S ($U - TS$) takes the minimum and hence the amount of diffusion is determined.

Below we use symbols introduced in Appendix 1. In the simple model adopted here for an abrupt junction (Fig. 6.4), the carrier density in the “depletion layer” caused by the diffusion-Coulomb force balance, is as low as n_i . Let the net voltage between the p and n layers V_{bi} , then the energy increase due to the transfer of an electron from the n layer to the p layer is eV_{bi} . As in eq.(3.19), the electron and the hole concentrations are $n_n \sim N_D$ in the n layer, from eq.(2.23) $n_p \sim n_i^2/N_A$ in the p layer respectively. The number of cases for putting $N_{1,2}$ electrons into two boxes with the site number N for each, is $W = {}_N C_{N_1} {}_N C_{N_2}$. If the transfer of electrons is limited between the two boxes, $dN_1 = -dN_2$ and in case of $N \gg N_{1,2}$, $d(\ln W) \approx \ln(N_2/N_1)dN_1$, which is well known as the entropy due to mixing of gases. We apply this general discussion to the above n- and p-layers, that is, $dN_1 = -1$, $N_1 = n_n$, $N_2 = n_p$. From the condition for the free energy to take a extremum $d(U - TS)/dn_n = 0$, we obtain

$$eV_{bi} = k_B T \ln \frac{n_n}{n_p} \sim k_B T \ln \frac{N_D N_A}{n_i^2} = E_g - k_B T \ln \frac{N_c N_v}{N_D N_A}, \quad (6.31)$$

where we put $n_n \sim N_D$ and $p_p \sim N_A$.

In equilibrium, the chemical potential (the Fermi level) should be constant throughout the junction, and that should be at the same level with that of bulk when we look at a very far point from the junction in n- or p-layer. From the above we can draw a schematic diagram as Fig.6.4(c). Let the widths of depletion layers w_p , w_n respectively for p and n layers, then the electric field $E(x)$ inside the depletion layers is

$$-\epsilon\epsilon_0 E(x) = N_A(2x + w_p) + N_D w_n \quad (x < 0), \quad N_A w_p + N_D(w_n - 2x) \quad (x \geq 0). \quad (6.32)$$

Here ϵ is the dielectric constant and V_{bi} is expressed as

$$V_{bi} = \int_{-w_p}^{w_n} (-E(x))dx = \frac{e}{\epsilon\epsilon_0} (N_D + N_A) w_n w_p = \frac{e}{\epsilon\epsilon_0} (N_D + N_A) \frac{N_D}{N_A} w_n^2 \quad \because w_n N_D = w_p N_A. \quad (6.33)$$

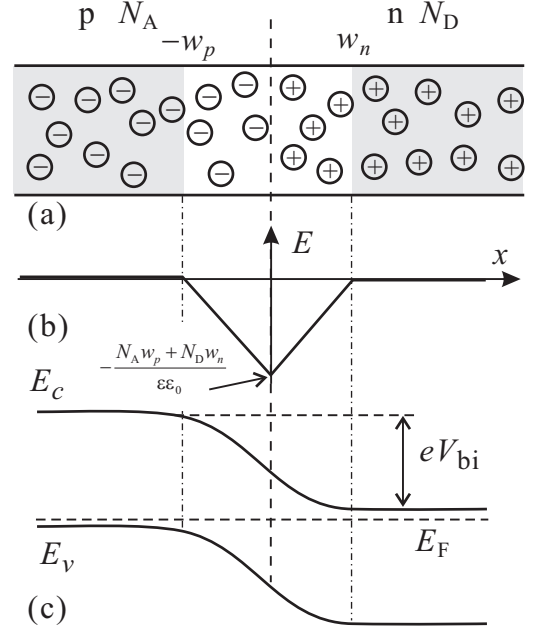


Figure 6.4: (a) Schematic cross section of an abrupt pn junction. (b) Electric field $E(x)$ across the depletion layer corresponding to the above. (c) Band diagram of the above pn junction.

The relation between the doping concentration and the width of the depletion layer is obtained from eq.(6.31) and eq.(6.33).

References

- [1] L. C. Lew Van Voon, M. Willatzen, “The k·p method” (Springer, 2009).
- [2] Chihaya Adachi, “Device physics of organic semiconductors” (Kodansya, 2012, in Japanese).
- [3] Minoru Imoto, “Practical introduction to molecular orbital” (Kagaku-dojin, 1986, in Japanese).
- [4] Seiichi Kagoshima, “One-dimensional electric conductors” (Shokabo, 1982, in Japanese).
- [5] W.P. Su, J.R. Schrieffer, and A.J. Heeger, Phys. Rev. Lett. **42**, 1698 (1979).